THE ASTROPHYSICAL JOURNAL, 169:63–86, 1971 October 1

LIGHT CURVES OF MIRA VARIABLES AT 1.04 MICRONS

G. W. LOCKWOOD
Kitt Peak National Observatory,* Tucson, Arizona
AND
ROBERT F. WING
Perkins Observatory, Ohio State and Ohio Wesleyan Universities
Received 1971 April 1; revised 1971 May 12

ABSTRACT

Near-infrared light curves have been compiled for twenty-five Mira variables of types M and S from photoelectric measurements of the radiation contained in a narrow bandpass near 1.04 μ. An average of twenty-seven observations per star was collected over a 5-year interval. The $I(104)$ magnitudes are almost completely free from molecular blanketing; the amplitudes at this wavelength are typically only 1.0 mag and never exceed 2.5 mag. Observations at the same phase in different cycles usually agree to within 0.1 mag, but differences as large as 0.5 mag have been recorded. Maximum light in $I(104)$ occurs approximately 0.1 period after visual maximum. Light curves at different infrared wavelengths with varying degrees of blanketing all have the same general character as the visual light curve of each star, although the amplitude depends upon the amount of blanketing.

Spectral types have been derived from measurements of TiO and VO bands made simultaneously with the measurements of $I(104)$. We give 595 spectral types for the twenty-two M and mild S stars and a judgment as to each star's most representative type at minimum light.

Pronounced humps on the rising branch, near phase 0.7, were observed in many stars; several stars have shown humps in some cycles but not in others. They cannot be attributed to changes in blanketing, since they are as evident in $I(104)$ as at other wavelengths and since the spectral type actually stays constant at its latest value during the rapid rise from minimum to secondary maximum. The rise from minimum seems to be associated with an increase in photospheric temperature, while the delay in the resulting dissociation of TiO and VO emphasizes the extreme stratification of these atmospheres.

I. INTRODUCTION

Few phenomena in astronomy have attracted and held the attention of so many observers, amateur and professional alike, as the light variations of long-period variable stars of the Mira type. A large part of this interest stems from the fact that the changes in brightness (and in spectrum) are qualitatively predictable but never *exactly* predictable, so that continual monitoring is necessary. During the past 50 years, members of the American Association of Variable Star Observers (AAVSO) have produced approximately 3 million estimates of the visual magnitudes of Mira variables; mean periods, mean light curves, and other information distilled from these data are given in Campbell (1955). Although all Mira variables show obvious cycle-to-cycle differences, each nonetheless possesses a distinctive mean light curve which differs significantly from those of most other Miras. The cycle-to-cycle differences themselves are not random: for example, bright and faint maxima tend to alternate, and bright maxima tend to occur ahead of schedule and to have earlier spectral types than faint maxima (see, e.g., Harrington 1965; Keenan 1966).

The light curve at each wavelength is the net effect of changes in temperature, radius, continuous opacity, and spectral features in both absorption and emission. The effect of TiO absorption upon the visual and photographic magnitudes of M-type Mira variables is strongly phase-dependent and often reaches several magnitudes (Smak 1964,

* Operated by the Association of Universities for Research in Astronomy, Inc., under contract with the National Science Foundation.

1966). We have long wondered whether some of the irregularities in the visual and photographic curves, and their failure to reproduce themselves, might not simply be the result of superficial distortions, by changing spectral features, of a more fundamental and regular continuum light curve. This idea can be tested by measuring continuum radiation, for example in the clear region near 1.04 μ recommended for this purpose by Wing (1967*a*). It will be shown here, however, that the brightness of the infrared continuum exhibits some of the same peculiarities and irregularities (but with smaller amplitude) as are seen in the heavily blanketed visual region. Some progress in interpreting the curves has nevertheless been possible as a result of collecting a large quantity of accurate, homogeneous data and measuring the spectral type corresponding to each point on the light curve.

Some important results have been obtained from previous infrared photometry of Mira variables with wide bandpasses. Photographic magnitudes at an effective wavelength of 8500 Å were measured by Hetzler (1936) for thirty Mira variables. His light curves have much smaller amplitudes than the corresponding visual light curves as a result of the longer wavelength and the decreased blanketing by TiO bands. The maxima on Hetzler's curves are reached at about the time of the visual maxima, but they persist longer. The cycle-to-cycle repetition is better than in the visual, but is clearly imperfect. The radiometric curves (which refer to all radiation transmitted by the Earth's atmosphere) published by Pettit and Nicholson (1933) for eleven Mira variables have still smaller amplitudes, and their maxima occur about 0.1 period after visual maximum. Pettit and Nicholson also constructed the bolometric light curve for the mean of six well-observed late-type Miras and found its maximum to occur slightly later still, at phase 0.14.

Mendoza V. (1967) has published a large number of observations on the Johnson (1966) system of wide-band multicolor photometry. With somewhat narrower filters, including one about 350 Å wide at 1.02 μ, Eggen (1967) has observed substantial segments of the light curves of several Mira variables.

Light curves of two Mira variables have been published in the narrow-band $I(104)$ magnitude used here. Wing (1967*a*) showed that the amplitude of χ Cyg in $I(104)$ was less than 2.5 mag in the 1965 cycle, when the V-amplitude exceeded 8.5 mag, and that the maximum in $I(104)$ showed the same phase lag as does the bolometric curve of Pettit and Nicholson (1933). A similar comparison of the $I(104)$ and V light curves, with similar results, was presented by Wing, Spinrad, and Kuhi (1967) for the Taurus infrared star (now known as IK Tau). In neither case, however, were observations from different cycles compared.

In this paper we discuss observations of $I(104)$ and spectral type that have been collected during the past 5 years for Mira variables of types M and S. Although more than 200 different Miras have been observed, we restrict attention here to the twenty-five variables with the most complete light curves.

II. OBSERVATIONS

a) The 27-Color and 5-Color Photometric Systems

Two different but related systems of narrow-band near-infrared photometry were used in this investigation. A 27-color system defined by means of a spectrum scanner was used by Wing at Lick Observatory from 1965 to 1968, and a 5-color system defined with interference filters has been used since 1969 by Lockwood at Kitt Peak National Observatory. The five filters all have close counterparts on the Lick system, although the filter are approximately 100 Å wide whereas a 30 Å bandpass was used with the scanner.

The Lick system measures the strengths of bands of CN, TiO, VO, and ZrO in the 7500–11000 Å region and defines the continuum quite well in most kinds of cool stars. Descriptions of this system and the observing procedures used are given in Wing (1967*b*)

and Wing *et al.* (1967). Since these papers were written, all 27-color observations have been formally reduced and transformed to the system of absolute fluxes given by Hayes (1970). With the exception of the most recent observations, all the data on the Lick system are contained in Wing's thesis (1967*c*). They are expressed as fluxes per unit wavelength interval on a magnitude scale, and the zero point of the whole system has been set by requiring that $I(104) = 0.00$ mag for Vega. Most of the observations were made with the 36-inch Crossley reflector, and some 120-inch measurements were kindly contributed by Dr. Hyron Spinrad.

The Kitt Peak observations were likewise mostly made with a 36-inch telescope. Five interference filters were selected to respond to some of the same spectral features as are measured on the Lick system. The characteristics of these filters, and the corresponding points on the Lick scanner program, are listed in Table 1. The designations given in column (1) are convenient abbreviations for the wavelengths. Filters 78, 88, and 105 are sensitive to the presence of TiO and VO bands, while filter 104 measures the $I(104)$ magnitude; the notations 104 and $I(104)$ can be used interchangeably. Filter 87, which is less affected by TiO than the first and third filters in stars earlier than M7, serves as a reference point for the measurement of the TiO index. Observations of infrared stars on this system have been published by Lockwood (1970) and Lockwood and McMillan (1971). The values of standard stars and the complete 5-color photometry of Mira variables can be found in Lockwood (1971).

After the Kitt Peak observations of different nights had been tied together by means of standard stars, they were transformed to the absolute scale of the Lick system. Since no significant color-dependent effects for stars in the spectral range O9–M5 could be found, the transformations simply involved the evaluation of the zero points, the standard errors in which were no greater than 0.003 mag. No rigorous tests for color terms could be made for very late type stars, all of which are variable, since no simultaneous observations were made with the two photometric systems. It is reasonable to suppose that systematic differences do exist between the Lick and the transformed Kitt Peak numerical results in the case of very late type stars in spectral regions broken by molecular bands. However, since we have not been able to establish the existence of any such systematic differences from actual comparisons of data, we conclude that they rarely exceed 0.05 mag at any of the five wavelengths. The internal standard errors of the magnitudes, within each system, are approximately ± 0.015 mag.

In the case of the $I(104)$ magnitude, with which this paper is primarily concerned, the transformations are particularly accurate because the spectra of M stars are quite clean

TABLE 1

PROPERTIES OF INTERFERENCE FILTERS

Designation (1)	Central Wavelength (Å) (2)	Width at Half Power (Å) (3)	Central Transmission (percent) (4)	Corresponding Point on Scanner Program* (Å) (5)	Feature Measured (6)
78.....	7817	90	66	7812	TiO
87.....	8778	82	69	8718	...
88.....	8884	114	50	8880	TiO
104.....	10351	125	51	10400	$I(104)$
105.....	10506	100	45	10564	VO

* 30 Å bandpass used on scanner program.

from 10250 to 10450 Å. The systematic error resulting directly from the shift in wavelength of 50 Å amounts to only 0.015 mag over the range of spectral type A0–M4, and an error of about the same size is expected over the range M4–M9. Such errors are inconsequential, and no corrections for them were applied. The total uncertainties in the $I(104)$ magnitudes for M stars should not exceed ± 0.03 mag, which is smaller than the symbols used in plotting the light curves. For S stars near minimum light, the errors of transformation are probably somewhat larger as a result of unidentified absorptions in this spectral region.

b) Spectral Types

Both photometric systems measure the strengths of the same TiO and VO bands. Although somewhat different numerical procedures have been developed for obtaining band-strength indices from the fluxes (see Wing 1967*c* and Lockwood 1971 for details), the spectral types in both cases are independent of interstellar reddening and are obtained from the sum of the TiO and VO indices, calibrated by means of the same standards of spectral type. For types M0–M8, we have relied upon the standard stars classified on the MK system by Keenan (1963), who likewise used both TiO and VO bands. A significant difference exists, however, between the spectroscopic and photometric classification systems in the case of Mira variables of types M5 and later in that Keenan (1966) uses the relative strengths of various bands while we use absolute strengths. For types later than M8, which are encountered only among Mira variables, we have followed the earlier recomendation of Wing (1967*b*), which has been widely adopted, of defining types M9.0 and M10 by *o* Cet at minimum and R Cas at minimum, respectively. Both stars have been found to attain somewhat different band strengths at the minima of different cycles, but better standards for these types have not been found.

The following spectral types are used in this paper: <M1, M1, M2, M3, M4.0, M4.5, M5.0, M5.5, M6.0, M6.5, M7.0, M7.5, M8.0, M8.2, M8.5, M8.8, M9.0, M9.2, M9.5, M9.8, M10.

Although the number of subdivisions increases with spectral type, so does the interval in band strength per subdivision. Each band-strength interval is several times as large as the pure observational uncertainty in the measured indices. The largest error in the spectral types given here, including possible systematic differences between the two systems, should be plus or minus one of the divisions listed above. The relatively low accuracy of our photometric types earlier than about M3 is a consequence of the weakness of the infrared TiO bands.

For the mild S star χ Cyg, in which TiO is much stronger than ZrO, we give "M equivalent" spectral types, determined exactly as for M stars. There is no evidence that our measurements of TiO and VO are contaminated by other absorptions in this star. For the pure (or nearly pure) S stars, however, we prefer not to attempt to give types of any kind, since unidentified bands (Keenan 1957; Wing 1967*c;* Spinrad and Wing 1969) appear near minimum light and affect the photometric TiO and VO indices.

c) Temperatures

Since the measurements at each wavelength are reduced to a system of absolute fluxes, it is possible to derive temperatures from the data. On the 27-color system, blackbody curves have been fitted to the best continuum points, and the resulting temperatures have been tabulated for all scans (Wing 1967*c*). For unreddened stars of types G0–M7.5, these temperatures have been found to match closely the effective temperatures whenever the latter are known. However, it is not possible to obtain accurate temperatures for M8–M10 stars on this system because only the region near 10400 Å remains free of serious blanketing. On the Kitt Peak system, absorption at the shortward continuum point, 87, becomes appreciable at a much earlier spectral type, about M5. The location of the continuum is also uncertain in cool S stars, on both

systems. Since good temperatures can be derived for fewer than 20 percent of the observations reported here, we have not included temperatures in the tables. A discussion of the temperatures of Mira variables derived from the 27-color scans is being prepared separately (Wing 1971), and in § IV we mention some temperature determinations that have been helpful in interpreting certain features of the light curves.

III. LIGHT CURVES

a) Computation of Phases

Since it is the purpose of this paper to combine observations made in different cycles, the method of computing the phases of observations must be chosen with care. The mean periods determined by the AAVSO and given in the *General Catalog of Variable Stars* (GCVS; Kukarkin *et al.* 1969), although preferable to the lengths of particular cycles, are not always adequate because changes in mean period are not uncommon. The epoch of zero phase, which by convention refers to the visual maximum, is particularly important to establish correctly in order that the phase shifts between visual and infrared maxima may be examined. For the present purposes, the phases must be referred to a period and epoch that represent the star's *average* behavior in *recent* years.

Light elements satisfying these criteria may be obtained conveniently from the predictions of the times of visual maxima published annually by the AAVSO (Mayall 1964–1970). We have solved simultaneously for the period and epoch which give the best fit, by the least-squares criterion, to all the predicted times of maximum occurring within the seven calendar years 1964–1970, during which our observations were made.

The twenty-five Mira variables which have been observed most extensively at both Lick and Kitt Peak are listed in Table 2. Column (2) gives the mean spectral type at normal maxima according to Table 8 of Keenan (1966); similarly, column (3) gives the type which, from the photometric measurements given below, is most representative of the star at minimum light. The types in columns (2) and (3) can thus be considered characteristics of the star determined from observations in many cycles. They are not, in general, the earliest and latest types that have been observed, as inspection of our individual results will quickly show (see Tables 3 and 5 below).

Column (4) gives the mean period listed in the GCVS. The last two columns give the recent elements, derived as described above and used in plotting the light curves. The derived periods are in good general agreement with the catalogued values, the differences exceeding 1 percent in only seven cases and never exceeding 2 percent. The largest apparent changes are for T Cep (decrease) and for V Cas and U Her (increases). R Aql is the only star in Table 2 with a well-documented history of period changes (Schneller 1965), and its mean period has apparently remained constant since 1954.

In the tables and light curves that follow, the cycles are numbered serially, with cycle 1 designating the cycle of the first infrared observations, which were made in 1965 (except for χ Cyg which begins with cycle 0, and R CVn which was first observed in January 1966). The cycle numbers as well as the phases are derivable from the elements in Table 2 by dividing the period into the number of days since the listed epoch (this yields the sum of cycle number and phase).

b) Light Curves of o Cet and T Cas in Six Colors

The photometry of o Cet (Mira) and T Cas at the five wavelengths of Lockwood's filter system is presented in Table 3. The entries are absolute fluxes per unit wavelength interval, on a magnitude scale. Observations made before JD 2440200 are Lick scanner observations extracted from the 27-color data; the remainder are Kitt Peak filter observations transformed to the Lick system, as explained in § II. The phases are based upon the light elements given in Table 2. For the Lick observations, the spectral types tabulated here are mostly taken from Wing (1967*c*) and thus are based upon the complete

TABLE 2

LIGHT-CURVE PROGRAM STARS

Star (1)	Spectral Type: Normal Maximum* (2)	Spectral Type: Normal Minimum (3)	Mean Period† (4)	Adopted Elements: Epoch (JD) (2438000+) (5)	Adopted Elements: Period (6)
R Aql	M6.5e	M8.5	293^{d}0	594.6	292^{d}2
R Aur	M6.5e:	M9.0	458.37	112.0	453.2
R Boo	M4.5e	M8.0	223.46	716.8	223.1
R Cam	S3, 7e	...	270.09	561.5	271.3
R CVn	M6.5e	M8.5	327.97	651.8	328.0
R Cas	M7e	M10	430.97	488.4	425.6
T Cas	M7.5e	M8.5	445.0	345.3	444.1
V Cas	M5.5e	M8.5	227.95	572.1	232.4
T Cep	M6.5e:	M8.5	387.79	369.1	381.9
o Cet	M5.5e	M9.0	331.65	455.6	333.4
R Cyg	S3, 9e	...	426.35	184.9	428.4
RT Cyg	M2.5e	M8.2:	190.24	686.5	189.1
χ Cyg	S7, 2e	M9.0	406.84	444.3	405.8
R Dra	M5e	M8.2	245.56	627.3	244.8
S Her	M5, Se	M8.5	307.60	619.8	305.6
U Her	M6.5e	M9.0	405.40	435.6	411.4
R Leo	M7e	M9.0:	312.57	579.8	309.3
R LMi	M7e	M8.8	372.28	392.6	368.6
W Lyr	M4.5e	M8.0	196.40	748.7	197.6
X Oph	M6.5e	M8.5	334.22	498.7	329.7
Z Oph	K4ep	M6.0	349.10	416.2	346.1
U Ori	M6.5e	M9.0	372.45	558.4	370.9
R Peg	M7e	M8.8	377.84	281.9	379.6
R Tri	M4e+	M8.2	266.40	531.4	266.7
S UMa	S0.5, 9e	...	225.89	536.3	225.3

* Keenan (1966). † Kukarkin *et al.* (1969).

27-color scans; the Kitt Peak types are believed not to differ systematically from the Lick types (see § II). To the right of the name of each star is given the full range of spectral type observed by us.

For comparison with the infrared light curves, photoelectric measurements of the V-magnitudes of o Cet and T Cas are collected in Table 4. Most of these were taken from Wing (1967*c*) and were obtained with the Lick Observatory 24-inch reflector and UBV photometer, but we also include values published by Johnson *et al.* (1966), Mendoza V. (1967), Landolt (1969), and Evans (1970). Several of the values listed are actually the means of two or more closely spaced observations by the same observer. The V-magnitudes of o Cet from cycle −1 (1963) and cycle 0 (1964) precede the first infrared measurements.

The light curves of o Cet and T Cas in V and the five infrared wavelengths are shown in Figures 1 and 2, respectively. The V curves are accompanied by the mean visual curves tabulated in Campbell (1955). It can be seen at a glance that the two stars have light variations of strikingly different character, and that this character is preserved at the different wavelengths. The hump on the rising branch of the AAVSO curve for T Cas appears also at the infrared wavelengths, including the continuum region measured by $I(104)$. No such feature appears in any of the curves for o Cet. The light curve of T Cas has a smaller amplitude than that of o Cet at each wavelength. The maximum at each infrared wavelength occurs after the visual maximum in both stars. The two stars differ greatly, however, in the phase of minimum light, which occurs near phase 0.62 in o Cet and phase 0.44 in T Cas, independent of wavelength.

TABLE 3

INFRARED OBSERVATIONS OF o CET AND T CAS

JD	Cycle	Phase	78	87	88	104	105	Spectral Type
			o Ceti	(M4.5-M9.2)				
2438990.0	1	0.60	2.64	1.59	1.46	-0.21	0.47	M8.8
39005.0	1	.65	-	-	1.58	-0.15	0.60	9.0
39013.0	1	.67	2.81	1.78	1.56	-0.19	0.58	9.0
39028.9	1	.72	2.73	1.71	1.22	-0.22	0.45	8.8
39040.9	1	.76	2.54	1.52	1.36	-0.25	0.40	8.8
39050.9	1	.79	2.36	1.33	1.23	-0.38	0.25	8.8
39058.9	1	.81	2.21	1.20	1.12	-0.40	0.22	8.8
39070.9	1	.85	1.96	0.95	0.96	-0.44	0.15	8.5
39091.8	1	.91	0.59	-0.14	-0.04	-0.76	-0.40	7.5
39097.8	1	.93	0.19	-0.47	-0.35	-0.95	-0.72	7.0
39101.8	1	.94	-0.05	-0.68	-0.53	-1.04	-0.87	6.5
39110.8	1	.97	-0.42	-1.01	-0.86	-1.17	-1.10	6.0
39165.6	2	.13	-0.46	-1.19	-1.04	-1.35	-1.34	5.5
39201.6	2	.24	0.37	-0.63	-0.47	-1.19	-1.12	7.5
39320.0	2	.59	2.77	1.61	1.45	-0.34	0.42	9.0
39334.0	2	.63	2.77	1.70	1.53	-0.31	0.53	9.2
39347.0	2	.67	2.75	1.68	1.47	-0.36	0.47	9.2
39370.0	2	.74	2.54	1.47	1.29	-0.44	0.27	9.0
39394.9	2	.82	2.08	0.97	0.89	-0.58	-0.04	8.8
39422.8	2	.90	0.54	-0.44	-0.32	-1.01	-0.89	7.5
39425.9	2	.91	0.33	-0.64	-0.47	-1.06	-1.01	7.0
39726.0	3	.81	2.03	1.04	0.93	-0.46	0.09	8.8
40104.0	4	.94	-0.02	-0.60	-0.47	-1.00	-0.76	7.0
40106.0	4	.95	-0.06	-0.62	-0.49	-1.02	-0.78	7.0
40263.6	5	.42	1.83	0.32	0.28	-0.79	-0.59	8.0
40277.6	5	.47	2.12	0.57	0.51	-0.65	-0.43	8.0
40433.9	5	.93	0.03	-0.79	-0.67	-1.00	-0.94	6.5
40452.9	5	.99	-0.74	-1.35	-1.22	-1.26	-1.30	5.0
40464.9	6	.03	-0.90	-1.45	-1.33	-1.33	-1.36	4.5
40481.9	6	.08	-0.86	-1.45	-1.34	-1.35	-1.40	4.5
40493.9	6	.11	-0.75	-1.44	-1.33	-1.37	-1.41	5.0
40518.8	6	.19	-0.33	-1.29	-1.17	-1.37	-1.40	5.5
40539.8	6	.25	0.14	-1.05	-0.93	-1.30	-1.34	6.0
40591.7	6	.41	1.41	-0.02	0.02	-0.88	-0.86	6.5
40617.7	6	.48	2.02	0.55	0.55	-0.58	-0.46	7.5
40633.6	6	.53	2.41	0.90	0.87	-0.39	-0.18	8.0
			T Cassiopeiae	(M6.0-M9.0)				
2439013.0	1	0.50	4.31	3.24	3.12	1.50	2.05	M8.8
39041.0	1	.57	3.87	2.80	2.75	1.33	1.78	8.5
39060.9	1	.61	3.45	2.37	2.38	1.12	1.47	8.2
39097.9	1	.69	3.20	2.18	2.24	1.10	1.36	8.0
39207.7	1	.94	2.76	1.81	1.87	1.06	1.11	7.0
39319.9	2	.19	3.75	2.51	2.51	1.07	1.36	8.2
39335.0	2	.23	3.92	2.67	2.69	1.19	1.54	8.2
39371.9	2	.31	4.33	3.12	3.02	1.32	1.89	8.8
39393.8	2	.36	4.54	3.37	3.21	1.50	2.12	8.8
39423.9	2	.43	4.69	3.54	3.35	1.56	2.30	9.0
39671.0	2	.99	2.61	1.59	1.71	0.86	0.99	7.0
40105.8	3	.96	2.69	1.65	1.79	0.97	1.09	7.5
40263.7	4	.32	4.57	2.91	2.83	1.49	1.71	8.0
40264.6	4	.32	4.59	2.95	2.87	1.52	1.73	8.0
40277.6	4	.35	4.74	3.08	2.99	1.61	1.85	8.0
40383.0	4	.59	4.17	2.52	2.48	1.28	1.52	8.2
40396.9	4	.62	3.86	2.22	2.22	1.14	1.34	8.2
40453.9	4	.75	3.18	1.70	1.75	0.99	1.10	8.0
40465.9	4	.78	3.20	1.72	1.78	1.03	1.12	7.5
40493.9	4	.84	3.30	1.85	1.90	1.14	1.24	7.5
40519.8	4	.90	3.15	1.75	1.81	1.12	1.17	7.0
40586.8	5	.05	2.51	1.23	1.31	0.80	0.78	6.0
40617.7	5	.12	2.89	1.53	1.59	0.90	0.90	6.5
40633.6	5	.15	3.11	1.70	1.78	0.97	0.99	7.0
2440706.0	5	0.32	4.42	2.85	2.84	1.53	1.72	M8.2

TABLE 4

VISUAL MAGNITUDES OF *o* CETI AND T CASSIOPEIAE

JD	Cycle	Phase	*V* (mag)
	o Ceti		
2438299.0	−1	0.53	8.03*
2438367.6	−1	0.74	8.12*
2438391.6	−1	0.81	7.09*
2438466.6	0	0.03	3.33*
2438480.6	0	0.07	3.51*
2438629.0	0	0.52	7.90
2438634.0	0	0.54	8.05
2438640.0	0	0.55	8.20*
2438647.0	0	0.58	8.46
2438651.9	0	0.59	8.44*
2438653.9	0	0.60	8.58
2438666.0	0	0.63	8.79
2438669.8	0	0.64	8.65*
2438676.9	0	0.66	8.68*
2438681.9	0	0.68	8.75*
2438801.6	1	0.04	3.40
2438821.6	1	0.10	3.09
2438964.0	1	0.52	8.57
2438978.0	1	0.57	8.97
2438988.0	1	0.60	9.01
2438993.0	1	0.61	9.18
2439014.0	1	0.67	9.25
2439018.9	1	0.69	9.12
2439023.9	1	0.70	9.24
2439039.9	1	0.75	8.89
2439059.8	1	0.81	8.51
2439062.9	1	0.82	8.30
2439095.8	1	0.92	4.50
2439099.7	1	0.93	4.09*
2439108.7	1	0.96	3.39
2439129.6	2	0.02	3.04*
2439165.7	2	0.13	3.59
2439199.7	2	0.23	5.24
2439322.0	2	0.60	9.21
2439336.0	2	0.64	9.45
2439348.0	2	0.68	9.49
2439363.0	2	0.72	9.27
2439371.0	2	0.74	9.09
2439385.0	2	0.79	8.63
2439393.0	2	0.81	8.35
2439420.9	2	0.89	5.75
2439421.9	2	0.90	5.58
2439448.7	2	0.98	3.64*
2439508.7	3	0.16	4.42
2439747.0	3	0.87	5.38†
2439752.0	3	0.89	5.20†
2439756.0	3	0.90	4.96†
2439766.0	3	0.93	4.60†
2439770.0	3	0.94	4.56†
2439785.0	3	0.99	4.12†
2439786.0	3	0.99	4.00†
2439810.0	4	0.06	3.24†
2440128.9	5	0.02	3.70‡
	T Cassiopeiae		
2438821.7	1	0.07	8.35
2438993.0	1	0.46	11.07
2439013.9	1	0.50	10.69
2439023.9	1	0.53	10.47
2439032.8	1	0.55	10.18*
2439039.9	1	0.56	10.02
2439053.9	1	0.59	9.61
2439056.7	1	0.60	9.52*
2439095.8	1	0.69	9.02
2439165.7	1	0.85	8.39
2439199.7	1	0.93	7.93
2439240.0	2	0.01	7.68
2439322.0	2	0.20	9.27
2439336.0	2	0.23	9.62
2439348.0	2	0.26	9.94
2439363.0	2	0.29	10.25
2439370.9	2	0.31	10.42
2439392.9	2	0.36	10.70
2439420.9	2	0.42	11.11
2439445.7	2	0.48	11.09*
2439508.7	2	0.62	9.77
2439657.0	2	0.95	7.85
2440128.7	4	0.02	7.46‡

* Catalina observations (Johnson *et al.* 1966; Mendoza V. 1967).
† Evans (1970). ‡ Landolt (1969).

Both stars show rather good cycle-to-cycle repetition in the infrared, better than that of the majority of the Miras we have studied. Different cycles are indicated by different symbols according to the scheme given in the caption of Figure 1. (The same correspondence between symbol and cycle number is used in all subsequent figures.) The greatest discordance between cycles in the infrared curves for *o* Cet occurs near phase 0.2 in the 78, 87, and 88 curves, where the two observations of cycle 2 (*open circles*) fall well below the series from cycle 6 (*open triangles*). The two sets of observations were made with different equipment, but the differences are larger than can be attributed to errors in transformation (see § II*a*) and must indicate real differences between the two cycles. In fact, the maximum of cycle 6 (1969) was exceptionally bright visually, the brightest

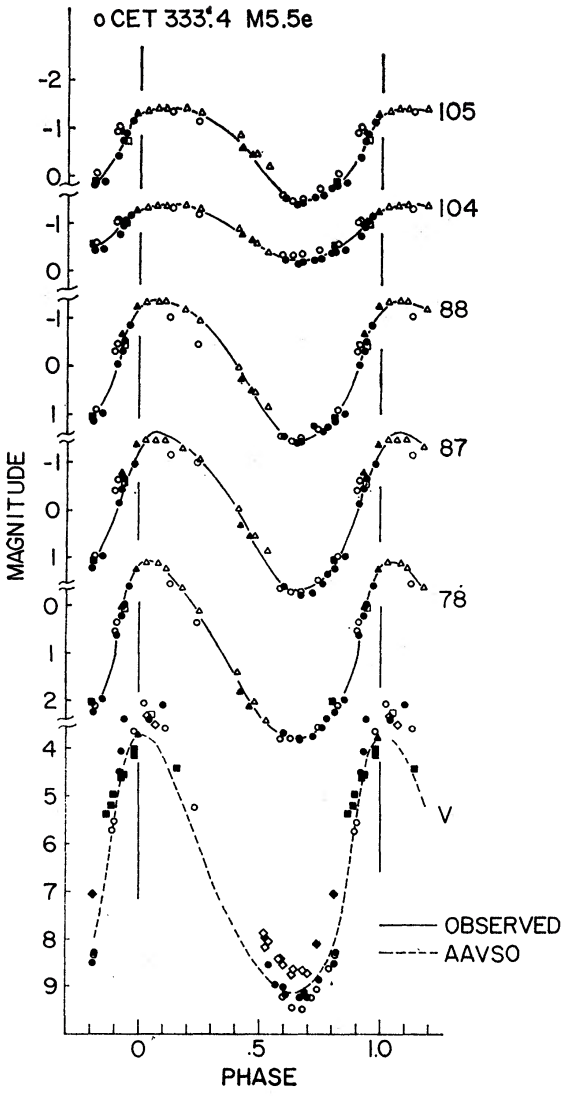

Fig. 1

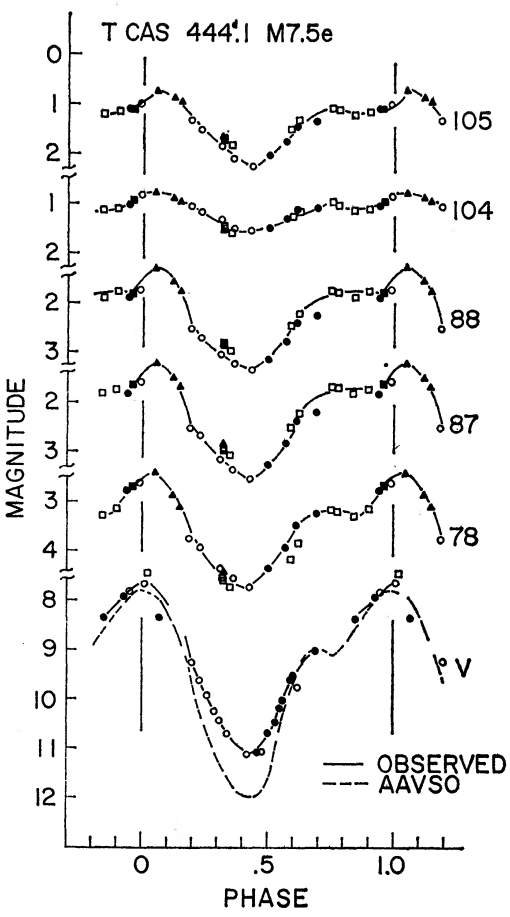

Fig. 2

Fig. 1.—Light curves of Mira (*o* Cet) in *V* and at the infrared program wavelengths. Wavelength designations to the right of the curves are defined in Table 1, and photometric data are from Tables 3 and 4. Cycles are numbered serially, the infrared observations starting with cycle 1 in 1965, and are coded as follows: −1 = ♦, 0 = ◇, 1 = ●, 2 = ○, 3 = ■, 4 = □, 5 = ▲, 6 = △, 7 = ▼, 8 = ▽, 9 = ♦, 10 = ◇.

Fig. 2.—Light curves for T Cas in six colors. Coded as in Fig. 1.

since 1906 (*Sky and Telescope* 1969). Note that *o* Cet also reached an unusually early spectral type (M4.5) at this maximum; the displacement of the points from cycles 2 and 6 is at least partly a direct result of the difference in TiO absorption. It is interesting that nearly the same continuum magnitude 104 was attained in cycles 2 and 6.

Many instances of substantial cycle-to-cycle differences are present in our data, even in the 104 curves. For example, the 104 curve for *o* Cet clearly indicates a difference in continuum brightness at minimum between cycles 1 and 2, both of which were observed at Lick. Surprisingly, a significantly later spectral type was reached at the brighter of the two minima (M9.2 compared with M9.0).

The V curve for o Cet shows much greater scatter than any of its infrared curves. At Lick Observatory, good coverage in V was obtained near the times of three consecutive minima. The 1964 minimum (*open diamonds*) was definitely brighter than the 1965 and 1966 minima. Of the observations near the 1964 minimum, five were made at Lick and five at the Catalina station of the Lunar and Planetary Laboratory (Johnson *et al.* 1966; Mendoza V. 1967), and it is noteworthy that no systematic differences between the two sets of equipment are evident. On the other hand, the fact that nearly all photoelectric V-magnitudes of o Cet and T Cas at bright phases lie above the AAVSO curves may indicate a systematic difference between the two kinds of visual magnitudes.

Both o Cet and T Cas have much smaller amplitudes in $I(104)$ than at the other wavelengths studied. This is generally true of Mira variables of types M and S and is a direct result of the freedom of $I(104)$ from molecular blanketing. The 78, 87, and 88 curves are depressed by TiO and the 105 curve by VO; the growth of these bands with decreasing temperature and decreasing continuum brightness serves to amplify the light variation. In o Cet, the brighter portions of the 104 and 105 curves have the same shape because the VO absorption is negligible at those phases, but the growth of VO toward minimum strongly depresses the lower portions of the 105 curve.

The effects of molecular blanketing upon the observed amplitudes can be checked quantitatively by means of the depressions measured with respect to blackbody continua fitted to the 27-color scans and tabulated in Wing (1967*c*). The VO depressions in o Cet range from zero at maximum light to 0.8 mag at minimum, causing the mean amplitude in 105, 1.9 mag, to be 0.8 mag greater than the mean amplitude of 1.1 mag in 104. The program wavelength most strongly depressed by TiO is 78, in which the amplitude of o Cet is about 3.3 mag in a typical cycle, or 2.2 mag greater than the 104 amplitude. Part of this difference is the direct result of the change in TiO absorption, and the remainder represents the change in the slope of the continuum between 78 and 104 as a result of the temperature change. There is some uncertainty in evaluating the relative importance of these two contributors because at minimum light the continuum is not well defined in the shortward half of the 27-color program. If, however, we adopt the result of Pettit and Nicholson (1933) that the temperature of o Cet at minimum is 1920° K and correct the continuum accordingly, then we find that the change in TiO blanketing at 78 is 1.1 mag while the remaining 1.1 mag corresponds to the (78 − 104) color change for a temperature varying from 1920° to 3100° K at maximum. The temperature of Mira variables at maximum are well determined on the 27-color program and are consistently much higher than the values given by Pettit and Nicholson (Wing 1967*c*, 1971).

The light curves of o Cet obtained photographically by Hetzler (1936) at an effective wavelength of 8500 Å agree well with our curves at 87 and 88 which are likewise affected by moderately strong TiO absorption. The amplitudes in 87 and 88 are about 2.9 mag in a typical cycle as compared with Hetzler's 2.8 mag. Hetzler observed the rising branch of o Cet in three cycles and found no trace of a hump, again in agreement with our data. He did not observe T Cas, but he did observe humps in the curves of several other stars, the best examples being χ Cyg and T Cep. On comparing his curves with the visual curves determined by the AAVSO, he remarked, "the infra-red curves, except for being shallower, correspond closely with the visual curves . . . shoulders or still-stands in the visual are duplicated in the infra-red." We have shown that his remark applies even to the infrared continuum.

On the other hand, the continuum curves in $I(104)$, with their smaller amplitudes and more pronounced phase lags of maximum light, resemble the radiometric curves of Pettit and Nicholson (1933) more closely than the near-infrared curves of Hetzler (1936). For o Cet, Pettit and Nicholson found a radiometric amplitude of 1.1 mag and a phase lag of about 0.12 period, both in excellent quantitative agreement with the $I(104)$ curve.

c) *Light Curves in I(104) for Twenty-three Additional Stars*

The preservation of the form of the light curve of each variable at the different wavelengths of our program, demonstrated above for *o* Cet and T Cas, is a property of the other well-observed Miras also. The continuum light curve at $I(104)$ contains nearly all the useful information concerning humps, phases of maximum and minimum, and cycle-to-cycle repetition that could be extracted from the complete set of light curves. Another kind of information—the difference in amplitude from filter to filter—is essentially that from which the spectral types have been derived. Therefore, we will present only the $I(104)$ magnitudes and spectral types for the remaining twenty-three stars of Table 2. These are given in the last two columns of Table 5 in which the stars are arranged alphabetically by constellation. Again, the cycle numbers and phases have been obtained from the elements given in Table 2. The spectral types from Lick observations (made prior to JD 2440200) have been derived from the complete 27-color data (Wing 1967*c*), while the Kitt Peak types are from 5-color observations given completely in Lockwood (1971). To the right of the name of each star in Table 5 appears the full observed range in the photometric spectral types. The three stars for which no types are listed are S stars.

i) *General Remarks concerning the Light Curves*

The $I(104)$ light curves for twenty-three Mira variables are shown in Figures 3–6. The stars have been arranged in order of increasing period in order to show any correlations that may exist between the form of the light curve and the period. Different symbols have been used for different cycles, as in the previous figures.

The amplitudes in $I(104)$ are quite small, typically only 1.0 mag, and they appear to be correlated with the period. A similar correlation exists between the visual amplitude and the period, both for these particular stars and for Miras in general (Merrill 1960). It should be emphasized, however, that there is substantial scatter in each of these correlations. The mean $I(104)$ amplitudes for the twenty-five stars studied, obtained by averaging the extrema of different cycles in a somewhat subjective fashion, are listed in Table 6. For comparison, we also list the mean visual amplitudes given in the "Remarks" to the GCVS, the mean range in a wide bandpass at 8500 Å measured by Hetzler (1936), and the mean range in the radiometric magnitude m_r from Table 3 of Pettit and Nicholson (1933). The ranges in $I(104)$ are similar to the ranges in radiometric magnitude. Whereas Hetzler's ranges are about one-half the visual ranges, the $I(104)$ and radiometric ranges are about one-fifth the visual ranges.

The following general remarks can be made on the basis of Figures 3–6:

1. All stars show cycle-to-cycle differences that are considerably greater than the errors of measurement and transformation. Most Miras repeat less faithfully than *o* Cet itself (Fig. 1). Typical differences are about 0.1 mag.

2. The largest cycle-to-cycle differences ($\sim$0.5 mag) have been found in χ Cyg and R Cas, both of which have unusually large amplitudes and periods greater than 400 days. The brightest $I(104)$ maxima of these stars were also bright visually and of abnormally early spectral types.

3. However, brighter-than-average maxima do not always correspond to spectral types that are earlier than average for maximum light. The same is true at other phases—i.e., whether a star is brighter or fainter than its average brightness at a given phase does not imply that its spectral type is earlier or later than average for that phase.

4. Humps on the rising branch of the light curve centered at about phase 0.7, discussed above in the case of T Cas (Fig. 2), are seen to be common phenomena. The majority of the stars studied have shown evidence of humps in at least some cycles. In a few stars the humps have accurately reproduced themselves (e.g., R Cam, T Cep), but

TABLE 5

I(104) MAGNITUDES AND SPECTRAL TYPES

JD	Cycle	Phase	I(104)	Spectral Type
R Aql	(M6.0-M8.5)			
2438950.9	1	0.22	$0^m.92$	M8.0
38985.8	1	.34	1.30	8.2
38993.8	1	.37	1.39	8.2
39012.7	1	.43	1.58	8.5
39020.8	1	.46	1.73	8.5
39028.8	1	.49	1.78	8.5
39041.7	1	.53	1.68	8.5
39058.7	1	.59	1.57	8.5
39070.7	1	.63	1.40	8.2
39097.6	1	.72	1.10	8.2
39202.1	2	.08	0.76	7.0
39237.0	2	.20	0.90	8.0
39319.9	2	.48	1.70	8.5
39328.8	2	.51	1.72	8.5
39333.9	2	.53	1.75	8.5
39345.8	2	.57	1.64	8.5
39356.8	2	.61	1.58	8.5
39369.8	2	.65	1.37	8.2
39393.7	2	.73	1.21	8.0
39422.7	2	.83	1.21	7.5
40018.0	4	.87	1.08	7.5
40339.0	5	.97	0.85	6.0
40345.0	5	.99	0.84	6.0
40349.9	6	.01	0.85	6.5
40358.9	6	.04	0.86	7.0
40367.9	6	.07	0.91	8.0
40382.9	6	.12	1.02	7.5
40395.9	6	.16	1.12	8.0
40403.9	6	.19	1.19	8.0
40433.8	6	.29	1.55	8.0
40493.7	6	.50	1.71	8.2
40518.6	6	.58	1.54	8.2
40528.6	6	.62	1.44	8.2
40705.9	7	.23	1.39	7.5
R Aur	(M6.0-M9.5)			
39018.0	1	.99	1.15	6.0
39098.0	2	.18	1.32	8.0
39164.9	2	.32	1.99	9.0
39201.9	2	.40	2.32	9.5
39237.7	2	.48	2.29	9.2
39335.0	2	.70	1.38	8.5
39373.0	2	.78	1.52	8.5
39394.0	2	.83	1.54	8.5
39423.0	2	.89	1.44	8.0
40264.7	4	.75	1.58	8.2
40465.0	5	.19	1.37	8.2
40495.0	5	.26	1.69	8.5
40539.8	5	.36	2.19	-
40586.8	5	.46	2.47	8.8
40617.8	5	.53	2.31	8.8
40633.8	5	.56	2.11	8.8
40705.7	5	.72	1.59	8.2
40839.0	6	.02	1.23	7.0
R Boo	(M2-M8.2)			
38993.7	1	.24	3.52	7.5
39165.1	2	.01	3.56	5.0
39208.0	2	.20	3.51	6.0
39237.0	2	.33	3.65	7.5
39262.9	2	.45	3.90	8.0
39319.8	2	.70	3.98	7.0
39334.7	2	.77	3.92	6.0
39356.7	2	.87	3.77	5.0
39371.7	2	.94	3.64	3
39394.7	3	.04	3.49	3
R Boo (cont.)				
2440264.0	6	0.94	$3^m.67$	M5.0
40278.0	6	.99	3.54	4.5
40297.9	7	.09	3.37	5.0
40316.9	7	.17	3.37	5.0
40326.8	7	.22	3.38	6.0
40327.8	7	.22	3.41	5.5
40339.8	7	.27	3.47	7.0
40344.8	7	.30	3.51	7.0
40349.9	7	.32	3.56	7.0
40367.7	7	.40	3.82	8.0
40382.7	7	.47	4.06	8.0
40395.7	7	.53	4.25	8.0
40403.7	7	.56	4.31	8.2
40481.6	7	.91	3.79	6.5
40618.9	8	.53	3.97	7.5
40632.9	8	.59	4.07	7.5
40662.9	8	.72	3.82	7.5
40695.8	8	.87	3.65	5.0
40705.7	8	.92	3.63	4.5
40730.8	9	.03	3.44	2
R Cam				
39041.8	1	.77	4.98	
39060.7	1	.84	4.97	
39262.9	2	.59	5.15	
39333.9	2	.85	4.92	
39345.8	2	.89	4.91	
39356.9	2	.93	4.89	
39371.8	2	.99	4.76	
39393.7	3	.07	4.56	
39422.7	3	.17	4.52	
40303.9	6	.42	5.08	
40326.8	6	.51	5.23	
40338.8	6	.55	5.19	
40344.8	6	.57	5.15	
40349.8	6	.59	5.13	
40367.7	6	.66	4.94	
40383.7	6	.72	4.86	
40395.7	6	.76	4.86	
40408.7	6	.81	4.90	
40481.6	7	.08	4.51	
40494.6	7	.13	4.47	
40618.9	7	.58	5.27	
40633.9	7	.64	5.11	
40661.8	7	.74	4.90	
40695.7	7	.87	4.99	
40705.7	7	.90	4.95	
40730.8	8	.00	4.79	
40763.7	8	.12	4.54	
R CVn	(M5.5-M8.5)			
39151.1	1	.52	2.95	8.5
39202.1	1	.68	2.62	8.5
39240.9	1	.80	2.37	8.2
39319.8	2	.04	1.98	6.0
39334.7	2	.08	1.94	6.5
39356.7	2	.15	1.97	7.0
39369.7	2	.19	1.98	7.5
39394.7	2	.26	2.12	8.0
39669.9	3	.10	1.98	7.0
40016.8	4	.16	1.97	7.0
40278.0	4	.96	2.12	5.5
40297.9	5	.02	1.96	5.5
40316.8	5	.08	1.91	6.0

TABLE 5 (continued)

JD	Cycle	Phase	I(104)	Spectral Type
R CVn (cont.)				
2440327.8	5	0.11	1.93	M6.0
40338.8	5	.14	1.94	7.0
40344.7	5	.16	1.96	7.0
40349.7	5	.18	1.98	7.0
40367.7	5	.23	2.08	7.5
40382.7	5	.28	2.20	7.5
40395.7	5	.32	2.33	8.0
40403.7	5	.34	2.41	8.0
40494.6	5	.62	2.72	8.5
40593.0	5	.92	2.24	7.5
40618.9	5	.99	2.00	6.0
40632.9	6	.04	1.91	5.5
40660.9	6	.13	1.94	6.5
40661.8	6	.13	1.91	6.5
40673.9	6	.16	1.97	7.0
40695.7	6	.23	2.16	7.5
40705.7	6	.26	2.27	7.5
40730.7	6	.34	2.55	8.0
R Cas	(M6.0-M10)			
39013.0	1	.23	0.25	8.8
39041.0	1	.30	0.45	9.0
39097.9	1	.43	0.80	9.5
39111.9	1	.46	0.91	9.5
39167.7	1	.60	1.58	9.8
39207.7	1	.69	0.69	9.2
39319.9	1	.95	-0.23	6.0
39328.9	1	.97	-0.25	6.0
39335.0	1	.99	-0.23	6.0
39346.0	2	.02	-0.27	6.0
39356.9	2	.04	-0.28	6.5
39371.9	2	.08	-0.30	6.5
39393.8	2	.13	-0.22	7.0
39423.9	2	.20	-0.01	7.0
39671.0	2	.78	1.30	9.8
40017.0	3	.59	1.28	10
40264.6	4	.17	0.24	7.5
40351.0	4	.38	1.20	8.8
40383.0	4	.45	1.57	9.2
40396.9	4	.48	1.70	9.5
40408.9	4	.51	1.81	9.8
40433.9	4	.57	1.92	10
40465.9	4	.65	1.79	9.8
40493.9	4	.71	1.61	9.8
40617.6	5	.00	0.28	8.5
40633.7	5	.04	0.29	8.5
40706.0	5	.21	0.68	8.5
40824.9	5	.49	1.42	10
V Cas	(M5.0-M8.5)			
38976.0	1	.74	3.03	8.0
39013.0	1	.90	2.85	6.5
39029.0	1	.97	2.78	5.5
39041.0	2	.02	2.70	5.0
39052.0	2	.06	2.66	5.0
39097.9	2	.26	2.65	7.0
39346.0	3	.33	2.65	8.0
39371.9	3	.44	2.83	8.2
39393.8	3	.54	3.18	8.5
39423.0	3	.66	3.22	8.2
40351.0	7	.65	3.09	8.5
40368.0	7	.73	3.00	8.5
40383.0	7	.79	3.06	8.5
40396.9	7	.85	3.07	8.5
40408.8	7	.90	3.00	8.5
40433.9	8	.01	2.78	6.5

JD	Cycle	Phase	I(104)	Spectral Type
V Cas (cont.)				
2440465.9	8	0.15	2.64	M6.0
40482.8	8	.22	2.67	7.0
40494.7	8	.27	2.76	8.0
40519.8	8	.38	3.13	8.0
40617.6	8	.80	3.10	8.5
40706.0	9	.18	2.72	6.5
T Cep	(M5.5-M8.8)			
39012.9	1	.69	0.20	8.2
39040.9	1	.76	0.25	8.2
39070.8	1	.84	0.25	8.0
39101.7	1	.92	0.17	7.5
39167.6	2	.09	0.09	7.5
39263.0	2	.34	0.70	8.5
39319.9	2	.49	0.65	8.8
39369.7	2	.62	0.20	8.2
39394.9	2	.69	0.17	8.0
39422.9	2	.76	0.21	8.0
40105.8	4	.55	0.41	8.5
40298.0	5	.05	0.13	5.5
40316.0	5	.10	0.16	6.5
40350.0	5	.19	0.30	7.0
40368.9	5	.24	0.30	8.0
40382.9	5	.27	0.31	8.0
40403.8	5	.33	0.35	8.2
40433.9	5	.41	0.45	8.5
40452.8	5	.46	0.56	8.2
40464.8	5	.49	0.55	8.2
40481.9	5	.53	0.55	8.2
40493.7	5	.56	0.46	8.2
40518.7	5	.63	0.25	8.0
40527.7	5	.65	0.17	8.0
40617.6	5	.89	0.05	6.0
40706.0	6	.12	0.20	6.5
R Cyg				
38975.9	1	.85	3.88	
38990.0	1	.88	3.81	
39004.8	1	.91	3.58	
39012.8	1	.93	3.45	
39040.8	1	.99	3.20	
39047.8	2	.01	3.18	
39060.7	2	.04	3.06	
39097.7	2	.13	3.01	
39237.9	2	.46	4.09	
39263.0	2	.52	4.35	
39328.8	2	.67	4.66	
39360.9	2	.75	4.08	
39390.8	2	.81	3.84	
39422.7	2	.89	3.48	
40316.0	4	.97	2.93	
40350.9	5	.06	2.89	
40368.9	5	.10	2.90	
40383.8	5	.13	2.92	
40518.7	5	.45	4.09	
40529.7	5	.47	4.23	
40763.9	6	.02	2.87	
RT Cyg	(M4.0-M8.8)			
38975.9	1	.53	5.14	7.5
39004.8	1	.68	5.03	7.5
39028.9	1	.81	4.90	6.5
39041.9	1	.88	4.78	5.0
39060.8	1	.98	4.59	4.0
39070.8	2	.03	4.54	4.0
39097.7	2	.17	4.46	4.5
39372.7	3	.63	4.99	6.5

TABLE 5 (continued)

JD	Cycle	Phase	I(104)	Spectral Type
RT Cyg (cont.)				
2440304.0	8	0.55	$5^m.26$	M8.2
40317.0	8	.62	5.33	8.5
40350.9	8	.80	5.13	8.5
40368.9	8	.90	4.99	8.2
40382.9	8	.97	4.76	7.5
40403.8	9	.08	4.44	6.5
40433.9	9	.24	4.45	7.0
40465.8	9	.41	4.78	8.5
40481.7	9	.49	5.00	8.5
40482.7	9	.50	5.01	8.8
40493.7	9	.56	5.08	8.5
40705.9	10	.68	5.22	8.2
χ Cyg	(M2-M9.0)			
38838.1	0	.97	-0.25	-
38892.0	1	.10	-0.38	-
38951.0	1	.25	0.18	8.0
38989.9	1	.34	0.73	8.8
39004.8	1	.38	0.96	8.8
39017.8	1	.41	1.23	9.0
39028.8	1	.44	1.50	9.0
39040.9	1	.47	1.69	9.0
39060.8	1	.52	2.03	8.8
39097.7	1	.61	1.65	8.8
39202.0	1	.87	0.77	8.0
39237.0	1	.95	0.38	5.5
39241.0	1	.96	0.35	6.0
39263.0	2	.02	0.31	6.0
39320.0	2	.16	0.31	7.5
39334.0	2	.19	0.42	8.2
39345.9	2	.22	0.54	8.5
39356.8	2	.25	0.66	8.8
39369.9	2	.28	0.78	8.8
39390.8	2	.33	1.03	8.8
39422.7	2	.41	1.46	9.0
39670.0	3	.02	-0.18	4.5
39725.9	3	.16	-0.03	7.0
40018.0	3	.88	0.22	7.5
40304.0	4	.58	1.61	8.8
40327.0	4	.64	1.33	8.8
40367.9	4	.74	0.47	8.5
40383.9	4	.78	0.35	8.2
40408.8	4	.84	0.23	8.2
40452.8	4	.95	-0.14	5.0
40464.7	4	.98	-0.28	3
40481.7	5	.02	-0.30	2
40493.7	5	.05	-0.30	3
40518.7	5	.11	-0.24	4.5
40529.7	5	.14	-0.20	5.0
40705.9	5	.57	1.62	9.0
R Dra	(M4.5-M8.5)			
38975.9	1	.42	4.15	8.2
39041.8	1	.69	3.95	8.2
39097.6	1	.92	3.86	6.0
39262.9	2	.60	4.42	8.5
39346.9	2	.94	3.86	6.5
39360.8	2	.99	3.71	5.5
39369.8	3	.03	3.65	5.0
39372.8	3	.05	3.65	5.0
39393.7	3	.13	3.54	5.5
39422.7	3	.25	3.68	7.0
40103.7	6	.03	3.66	5.5
40264.0	6	.69	4.26	8.0
40278.0	6	.74	4.14	8.0
40299.0	6	.83	3.95	8.0
40316.9	6	.90	3.76	6.0
40326.9	6	.94	3.75	5.0

JD	Cycle	Phase	I(104)	Spectral Type
R Dra (cont.)				
2440338.9	6	0.99	$3^m.62$	M4.5
40344.8	7	.02	3.59	5.0
40350.9	7	.04	3.64	4.5
40358,9	7	.07	3.59	5.5
40367.8	7	.11	3.60	5.5
40382.8	7	.17	3.62	6.5
40395.8	7	.22	3.65	7.0
40403.8	7	.26	3.65	7.5
40464.7	7	.51	4.12	8.0
40481.7	7	.58	4.17	8.0
40482.6	7	.58	4.18	8.0
40493.7	7	.62	4.13	8.2
40619.0	8	.14	3.70	5.0
40705.8	8	.49	4.29	8.2
40745.9	8	.65	4.26	8.5
S Her	(M2-M8.8)			
38985.8	1	.20	2.94	7.0
39040.7	1	.38	3.38	8.5
39237.0	2	.02	2.91	2
39241.0	2	.03	2.93	3
39320.8	2	.29	3.31	8.0
39334.8	2	.34	3.42	8.2
39356.8	2	.41	3.65	8.8
39394.7	2	.54	3.80	8.8
39423.6	2	.63	3.65	8.2
40315.9	5	.55	3.85	8.2
40326.9	5	.59	3.72	8.0
40339.9	5	.63	3.37	8.0
40350.8	5	.66	3.22	8.0
40368.8	5	.72	3.18	7.5
40408.7	5	.85	3.27	6.5
40453.7	6	.00	3.00	4.0
40464.7	6	.04	2.88	3
40481.7	6	.09	2.81	3
40494.7	6	.14	2.78	4.5
40619.0	6	.54	3.61	8.0
40705.8	6	.83	3.26	6.5
U Her	(M7.5-M9.5)			
38975.8	1	.31	1.92	8.0
38993.8	1	.36	2.12	8.2
38041.7	1	.47	2.38	8.8
39060.6	1	.52	2.69	9.2
39208.1	1	.88	2.24	9.5
39237.0	1	.95	1.58	9.0
39320.8	2	.15	1.52	8.8
39333.8	2	.18	1.61	9.0
39356.8	2	.24	1.76	8.8
40105.7	4	.06	1.36	8.0
40315.9	4	.57	2.73	8.8
40338.9	4	.63	2.74	8.8
40349.9	4	.65	2.69	8.8
40368.8	4	.70	2.58	8.8
40383.8	4	.74	2.45	8.5
40395.8	4	.76	2.38	8.8
40403.7	4	.78	2.36	8.8
40481.6	4	.97	1.46	8.0
40518.6	5	.06	1.27	7.5
40619.0	5	.31	1.83	8.0
40705.8	5	.52	2.61	8.5
40745.9	5	.62	2.72	8.8

TABLE 5 (continued)

JD	Cycle	Phase	I(104)	Spectral Type
R Leo	(M6.0-M9.2)			
2439071.1	1	0.59	$0^m.15$	M9.2
39098.1	1	.68	-0.11	9.2
39112.0	1	.72	-0.27	9.2
39151.0	1	.85	-0.55	9.2
39165.0	1	.89	-0.65	9.0
39201.9	2	.01	-0.91	8.2
39237.8	2	.13	-0.79	8.5
39510.0	3	.01	-0.98	7.0
40016.7	4	.65	-0.08	8.8
40263.9	5	.44	0.04	8.0
40277.8	5	.49	0.14	8.0
40297.8	5	.55	0.27	8.0
40315.7	5	.61	0.22	8.5
40326.7	5	.65	0.11	8.5
40338.7	5	.69	0.00	8.2
40344.7	5	.71	-0.10	8.2
40350.7	5	.73	-0.20	8.2
40368.7	5	.78	-0.34	8.2
40383.7	5	.83	-0.38	8.2
40494.0	6	.19	-0.61	7.0
40519.0	6	.27	-0.43	7.5
40586.9	6	.49	0.02	8.2
40616.9	6	.59	-0.10	8.2
40632.9	6	.64	-0.30	8.2
40660.8	6	.73	-0.60	8.2
40661.7	6	.73	-0.59	8.0
40674.7	6	.77	-0.62	8.0
40695.7	6	.84	-0.63	7.5
40705.7	6	.87	-0.68	7.5
40730.7	6	.95	-0.85	6.0
R LMi	(M6.5-M9.0)			
39098.1	1	.91	1.22	7.5
39151.0	2	.06	1.13	7.0
39165.0	2	.10	1.16	7.5
39201.9	2	.20	1.34	8.0
39240.8	2	.30	1.60	8.2
39319.7	2	.52	2.13	9.0
39424.1	2	.80	1.34	8.8
39510.1	3	.03	1.05	7.5
40263.9	5	.08	1.18	6.5
40277.8	5	.11	1.16	6.5
40297.8	5	.17	1.26	6.5
40315.7	5	.22	1.35	7.0
40326.7	5	.25	1.39	7.5
40339.7	5	.28	1.57	7.0
40350.7	5	.31	1.69	7.5
40368.7	5	.36	1.90	8.0
40383.7	5	.40	2.09	8.0
40519.0	5	.77	1.78	8.2
40592.9	5	.97	1.38	7.0
40601.0	5	.99	1.31	6.5
40617.9	6	.04	1.27	6.5
40632.9	6	.08	1.24	6.5
40660.8	6	.15	1.33	7.0
40661.7	6	.16	1.35	7.0
40672.7	6	.19	1.41	7.0
40674.7	6	.19	1.42	7.0
40695.7	6	.25	1.56	7.0
40705.7	6	.28	1.61	7.5
40730.7	6	.34	1.83	8.0

JD	Cycle	Phase	I(104)	Spectral Type
W Lyr	(M2-M8.0)			
2438950.9	1	0.02	$4^m.92$	M4.5
38970.9	1	.12	4.79	5.0
38989.8	1	.22	4.78	5.0
39012.8	1	.34	4.83	6.5
39028.7	1	.42	4.91	7.5
39040.8	1	.48	5.14	8.0
39047.7	1	.51	5.23	8.0
39102.6	1	.79	5.06	6.0
40299.0	7	.85	5.08	6.0
40316.0	7	.93	5.08	5.0
40326.9	7	.99	4.96	4.0
40339.0	8	.05	4.97	4.0
40344.9	8	.08	4.95	4.0
40349.9	8	.10	4.95	4.0
40357.9	8	.14	4.91	4.5
40367.9	8	.19	4.87	5.0
40382.9	8	.27	4.91	5.5
40396.8	8	.34	4.98	7.0
40403.9	8	.38	5.00	8.0
40433.9	8	.53	5.10	8.0
40464.7	8	.68	4.92	6.0
40705.9	9	.90	5.09	5.5
40745.8	10	.11	4.88	2
40763.9	10	.20	4.81	4.0
X Oph	(M7.0-M8.5)			
38985.8	1	.48	1.40	8.5
39012.7	1	.56	1.36	8.2
39028.8	1	.61	1.25	8.2
39047.7	1	.67	1.16	8.0
39070.7	1	.73	1.06	8.0
39101.6	1	.83	1.00	7.5
39168.1	2	.03	0.81	7.0
39237.0	2	.24	1.09	8.2
39319.9	2	.49	1.35	8.5
39333.9	2	.53	1.29	8.5
39345.8	2	.57	1.18	8.2
39371.7	2	.65	0.97	8.2
39422.7	2	.80	1.02	7.0
40316.0	5	.51	1.54	8.2
40339.9	5	.58	1.38	8.2
40349.9	5	.61	1.31	8.2
40368.9	5	.67	1.19	8.2
40383.8	5	.72	1.13	8.0
40396.8	5	.76	1.11	8.0
40403.9	5	.78	1.08	8.0
40433.9	5	.87	1.05	7.5
40452.8	5	.93	0.94	7.0
40453.8	5	.93	0.95	7.0
40464.7	5	.96	0.86	7.0
40481.7	6	.01	0.86	7.5
40493.7	6	.05	0.87	8.0
40518.6	6	.13	0.93	8.0
40528.6	6	.16	0.94	8.0
40705.9	6	.69	1.17	8.0
40784.8	6	.93	0.88	7.0
Z Oph	(< M1-M7.5)			
38975.8	1	.62	6.21	5.5
38989.7	1	.66	6.20	5.5
39028.7	1	.77	5.93	4.5
39047.7	1	.82	5.85	4.5
39241.0	2	.38	5.77	4.5

TABLE 5 (concluded)

JD	Cycle	Phase	I(104)	Spectral Type
Z Oph (cont.)				
2439319.9	2	0.61	$6^m.27$	M6.0
39334.8	2	.65	6.18	6.0
39372.7	2	.76	6.01	4.5
39391.6	2	.82	5.86	3
39422.6	2	.91	5.54	<1
40338.9	5	.56	6.21	5.5
40349.9	5	.59	6.22	5.5
40367.8	5	.64	6.27	5.5
40382.8	5	.68	6.23	5.0
40396.7	5	.72	6.15	4.5
40408.7	5	.76	5.97	4.0
40482.6	5	.97	5.38	<1
40518.6	6	.07	5.25	<1
40526.6	6	.10	5.18	<1
40708.9	6	.62	6.32	7.5
U Ori (M7.5-M9.0)				
39042.0	1	.30	1.21	8.2
39062.0	1	.36	1.32	8.2
39102.0	1	.47	1.78	8.5
39150.9	1	.60	2.19	9.0
39165.8	1	.64	2.18	9.0
39207.8	1	.75	1.83	8.5
39236.7	1	.83	1.65	8.5
39347.0	2	.13	0.90	7.5
39372.0	2	.19	0.93	8.0
39423.1	2	.33	1.22	8.5
40263.7	4	.60	2.14	8.8
40264.7	4	.60	2.15	8.8
40277.7	4	.64	2.13	8.8
40298.7	4	.69	1.99	9.0
40316.7	4	.74	1.83	9.0
40339.6	4	.80	1.68	9.0
40466.0	5	.14	0.95	8.2
40483.0	5	.19	0.99	8.2
40494.0	5	.22	1.02	8.2
40539.8	5	.34	1.38	8.5
40586.0	5	.47	1.81	8.8
40600.8	5	.51	1.93	9.0
40618.8	5	.56	2.06	9.0
40633.7	5	.60	2.10	9.0
40661.7	5	.67	1.94	8.8
40705.7	5	.79	1.54	8.5
R Peg (M5.5-M9.0)				
38989.9	1	.87	2.20	9.0
39028.9	1	.97	1.78	7.5
39040.9	1	.99	1.71	6.5
39047.9	2	.02	1.76	7.0
39050.9	2	.03	1.74	7.0
39060.9	2	.05	1.69	7.0
39091.8	2	.13	1.75	7.5
39101.7	2	.16	1.78	7.5
39263.0	2	.58	2.77	8.8
39320.0	2	.73	2.20	8.5
39334.0	2	.77	2.09	8.5
39372.9	2	.87	2.11	8.2
39393.9	2	.93	2.02	7.5
39422.8	3	.01	1.84	5.5
39425.9	3	.01	1.83	5.5
40369.0	5	.50	2.82	8.5
40382.9	5	.53	2.94	8.5
40396.9	5	.57	2.93	8.5
40403.9	5	.59	2.92	8.8
40465.9	5	.75	2.38	8.5
40482.8	5	.80	2.22	8.2
40494.7	5	.83	2.15	8.2
40519.8	5	.90	2.15	8.2

JD	Cycle	Phase	I(104)	Spectral Type
R Peg (cont.)				
2440586.6	6	0.07	$1^m.74$	M6.0
40617.6	6	.15	1.82	6.5
R Tri (M3-M8.5)				
38994.0	1	.73	2.67	7.0
39033.0	1	.88	2.63	5.0
39041.9	1	.91	2.62	4.0
39051.0	1	.95	2.47	3
39061.0	1	.99	2.42	3
39070.9	2	.02	2.41	3
39097.9	2	.12	2.30	4.5
39167.7	2	.39	2.77	8.0
39207.7	2	.54	3.08	8.5
39320.0	2	.96	2.49	5.0
39335.0	3	.01	2.36	5.0
39347.0	3	.06	2.29	5.5
39357.0	3	.10	2.32	-
39373.0	3	.16	2.30	7.0
39423.0	3	.34	2.66	8.2
40103.9	5	.90	2.71	5.5
40263.7	6	.50	3.04	6.5
40264.7	6	.50	3.07	7.0
40298.7	6	.63	3.02	7.5
40304.6	6	.65	2.93	7.5
40433.9	7	.13	2.29	4.5
40453.9	7	.21	2.33	6.0
40465.0	7	.25	2.39	6.5
40482.9	7	.32	2.60	7.0
40494.8	7	.36	2.75	7.5
40518.8	7	.45	3.03	8.0
40527.8	7	.49	3.12	8.0
40538.8	7	.53	3.19	8.2
40560.8	7	.61	3.23	8.2
40592.7	7	.73	2.99	8.5
40617.7	7	.82	2.81	8.5
40633.7	7	.88	2.78	8.2
40673.6	7	.03	2.44	6.0
S UMa				
38970.8	1	.93	4.90	
38989.7	2	.01	4.65	
39112.1	2	.56	5.31	
39166.0	2	.79	5.13	
39202.0	2	.95	4.81	
39240.9	3	.13	4.43	
39320.8	3	.48	5.33	
40298.9	7	.82	5.09	
40316.7	7	.90	5.02	
40326.7	7	.95	4.90	
40338.7	8	.00	4.72	
40344.7	8	.03	4.66	
40349.7	8	.05	4.57	
40357.7	8	.08	4.53	
40368.8	8	.13	4.46	
40383.7	8	.20	4.45	
40396.7	8	.26	4.55	
40593.0	9	.13	4.61	
40603.0	9	.17	4.59	
40618.0	9	.24	4.59	
40633.0	9	.31	4.74	
40661.9	9	.43	5.07	
40673.8	9	.49	5.18	
40695.7	9	.58	5.43	
40705.7	9	.63	5.30	

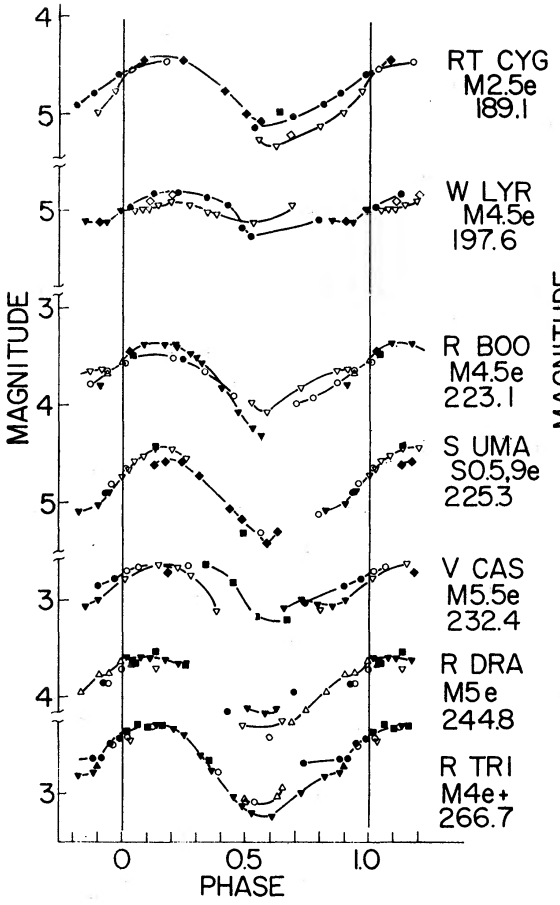

FIG. 3

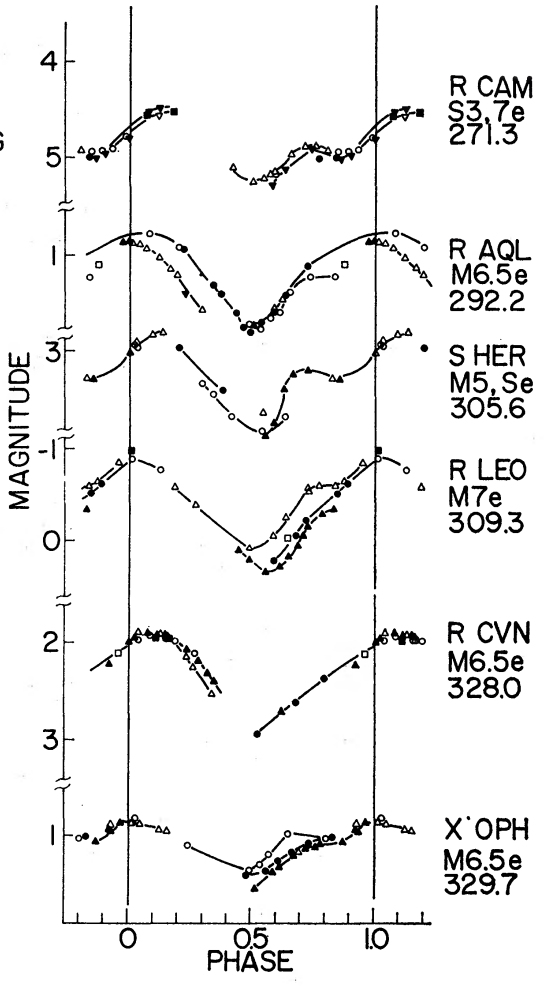

FIG. 4

FIG. 3.—Light curves in $I(104)$ for Mira variables in the period range 189^d–266^d. Photometric data and corresponding spectral types are given in Table 5. Below the name of each star appears the mean spectral type at maximum light from Keenan (1966) and the period used in calculating the phases (see Table 2). Light cycles are coded as in Fig. 1.

FIG. 4.—Light curves in $I(104)$ for Mira variables in the period range 271^d–329^d. Coded as in Fig. 1.

more commonly the cycle-to-cycle differences are greater in the phase interval 0.6–0.8 than in other parts of the light curve. During the flat part of the hump, the spectral type generally continues to decrease.

5. Maximum light in $I(104)$ occurs near phase 0.1 or 0.2 in most of these stars.

6. Minimum light in $I(104)$ occurs near phase 0.6 on the average, but it tends to occur at an earlier phase in stars with a hump on the rising branch. The phases of the visual minima (Campbell 1955) and the $I(104)$ minima do not seem to differ systematically.

7. The data of Table 5 show that each star's earliest spectral type has nearly always been recorded between phases 0.95 and 0.15, and usually very close to phase 0.00. Between the phase of visual maximum and the phase of infrared maximum, the spectral type usually advances substantially.

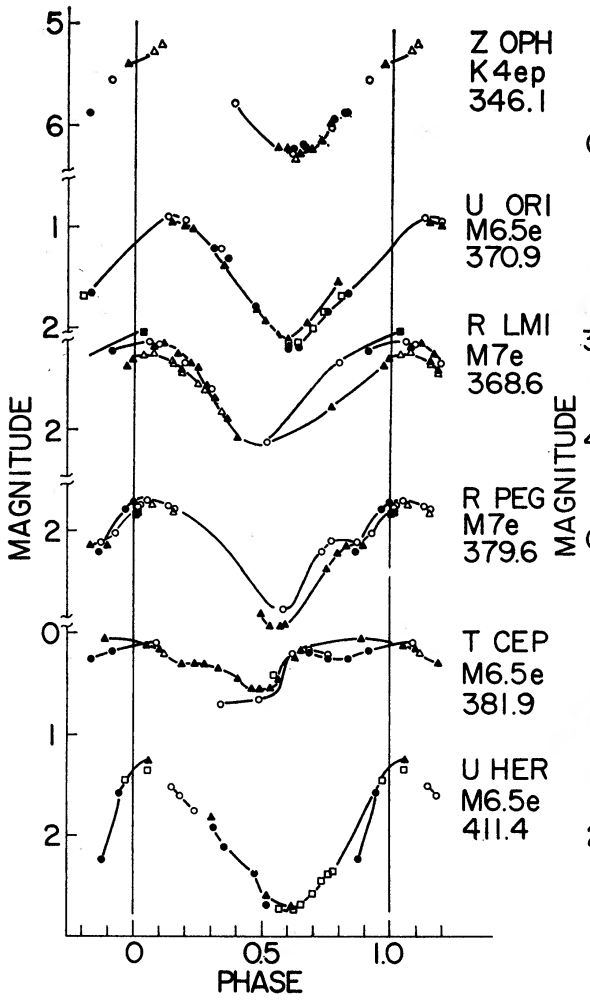

FIG. 5

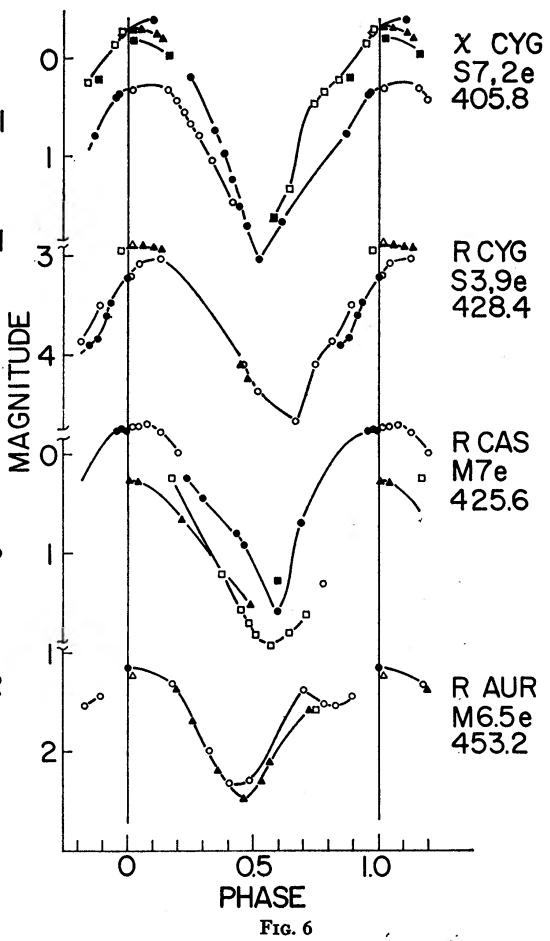

FIG. 6

FIG. 5.—Light curves in $I(104)$ for Mira variables in the period range 346^d–411^d. Coded as in Fig. 1.
FIG. 6.—Light curves in $I(104)$ for Mira variables in the period range 405^d–453^d. Coded as in Fig. 1.

8. The latest spectral type is usually reached close to the time of minimum light but is retained for perhaps 0.2 period while the $I(104)$ magnitude brightens rapidly. That is, the recovery from minimum occurs sooner in brightness than in spectral type.

ii) *Notes on Individual Stars*

Each Mira variable is an individual whose behavior cannot be specified simply by a few quantities such as period, amplitude, and mean type at maximum. In this section we bring in additional information concerning several of the stars and draw attention to some specific features in the light curves which illustrate both normal and abnormal behavior. We will discuss eleven of the stars in the order that their light curves appear in Figures 3–6.

RT Cygni.—This high-velocity, weak-lined Mira shows some spectroscopic evidence of high luminosity (Pettit 1944; Keenan 1966). The displacement between the two observed rising branches is unusually large (0.2 mag). The earliest recorded spectral type, M4.0, occurred near phase 0.0 when the temperature was ~3800° K, corresponding to a normal giant of type K5. From the spectroscopic types catalogued by Keenan

TABLE 6

COMPARISON OF MEAN AMPLITUDES

Star	V*	8500 Å†	m_r‡	I(104)
R Aql	5.4	2.6	0.91	0.90
R Aur	5.6	...	...	1.20
R Boo	5.1	...	...	0.75
R Cam	4.9	1.7	...	0.75
R CVn	4.2	...	...	1.00:
R Cas	5.6	2.9	...	1.65:
T Cas	4.0	...	...	0.70
V Cas	4.3	...	...	0.55
T Cep	4.3	2.2	...	0.55
o Cet	5.9	2.8	1.11	1.10
R Cyg	6.4	...	1.39	1.55:
RT Cyg	4.5	...	...	0.75
χ Cyg	8.2	4.0	1.14	2.00:
R Dra	4.8	2.3	...	0.65
S Her	5.0	...	...	0.90
U Her	5.0	...	...	1.35
R Leo	4.2	2.4	0.90	1.10
R LMi	5.5	...	0.95	0.95
W Lyr	4.3	2.1	...	0.35
X Oph	2.0	...	0.74	0.55
Z Oph	4.6	...	...	1.00
U Ori	5.7	...	...	1.20
R Peg	5.4	...	...	1.15
R Tri	5.5	2.5	0.85	0.85
S UMa	3.9	1.7	...	0.85
Mean	5.0	2.5	1.00	0.97

* Kukarkin *et al.* (1969).
† Hetzler (1936).
‡ Pettit and Nicholson (1933).

(1966), as well as our photometry, we judge the mean type at a normal maximum to be M4e rather than the value M2.5e given by Keenan.

W Lyrae.—The amplitude is unusually small, especially in cycle 8 (but see also V Cas, X Oph, and T Cep). The range in spectral type is nevertheless quite substantial in both cycle 1 and cycle 8: between phases 0.0 and 0.5, while the I(104) magnitude stays nearly constant, the type advances from about M4 to about M8.

R Trianguli.—The I(104) curve shows remarkably good cycle-to-cycle repetition, with seven cycles represented, except near phase 0.7 where there is a more pronounced hump in one cycle than in another. The variable R Tri is similar to RT Cyg in being much hotter than the TiO band strength suggests. It executed a well-defined loop in the (TiO, temperature)-plane in passing through the maximum of cycles 1–2 (Spinrad and Wing 1969, Fig. 9).

R Camelopardalis.—The light curve clearly shows a hump at phase 0.7 in at least two cycles, although no such feature appears in the mean visual curve (Campbell 1955). Nassau (1964) has called attention to the fact that the ZrO bands in this S star are stronger than the TiO bands at maximum light, but weaker than the TiO bands at minimum. The Lick scans, which measure both molecules, show that the ZrO bands are relatively insensitive to temperature while the TiO bands, in agreement with Nassau's results, range from virtual disappearance at maximum to a strength corresponding to M7.5 at minimum.

R Aquilae.—The period has decreased from about 350^d at the turn of the century to

293^{d}0 since 1954 (Ahnert 1964, 1965; Schneller 1965). The value 292^{d}2 used here, based on recent visual maxima, gives a good fit for the infrared minima; a period of 285^d would bring the two declining branches into agreement but would upset the fit at minimum. Spectroscopically R Aql is quite a normal Mira variable, although it is a source of OH radio lines (Wilson, Barrett, and Moran 1970) and the microwave water line (Turner *et al.* 1970, in which the star is identified only as IRC+10406).

S Herculis.—This star is noteworthy for the large hump observed in cycle 5 and the wide range in spectral type (M2–M8.8) recorded in cycle 2. The type M2 is much earlier than any observed by Keenan (1966) and occurred when the visual magnitude was the brightest ever recorded, measured photoelectrically at $V = 6.83$ (Wing 1967*c*). The $I(104)$ magnitude, however, does not seem to have been abnormally bright at that time.

X Ophiuchi.—This star is important as a visual binary showing some orbital motion; its mass has been estimated by Fernie (1959). The small mean visual amplitude, only 2.0 mag, is partly the result of the proximity of the K-type companion, but the $I(104)$ curve, on which the influence of the companion should be negligible, shows that X Oph is indeed a small-amplitude Mira.

Z Ophiuchi.—At maximum light, the TiO bands usually disappear completely and the atomic lines are greatly weakened (Merrill, Deutsch, and Keenan 1962, Figure 8). The $I(104)$ light curve, however, is very similar to that of the much cooler variable U Ori, appearing just below Z Oph in Figure 5. Several minima have been observed, the type at minimum ranging from M5.0 to M7.5. Wyckoff (1970) has noted that the near-infrared spectrum of Z Oph is peculiar in that different TiO bands suggest different spectral types.

T Cephei.—The $I(104)$ curve has a unique shape among the stars studied here, as well as a surprisingly small amplitude for a star with such a long period. There is some evidence (§ II*a*) that the period is decreasing. The mean visual curve (Campbell 1955) shows a slight hump on the rising branch.

χ *Cygni.*—This star is famous for having the largest visual amplitude of any well-observed Mira variable, and it also has the largest range in $I(104)$ that we have recorded (2.33 mag). The curve for cycle 1 (*filled circles*) in 1965 was shown previously in Wing (1967*a*), where it is compared with the concurrent V curve, also obtained photoelectrically. The 1965 maximum was a bright one, reaching $V = 4.11$. The subsequent maximum of 1966 reached only $V \approx 5.9$ and was also 0.5 mag fainter in $I(104)$. The two Lick series of observations are well displaced from one another not only in $I(104)$ but also in the diagram of band strength versus temperature, shown in Figure 9 of Spinrad and Wing (1969).

R Cassiopeiae.—Like χ Cyg, R Cas has both a large amplitude and major differences in magnitude between one infrared maximum and another. The bright maximum shown in Figure 6 was the brightest ever observed visually, reaching $V = 4.94$ in July 1966 (Wing 1967*c*). At minimum light, R Cas has stronger VO bands than any other star discussed in this paper, and we have used its spectrum at minimum to define spectral type M10 (Wing 1967*b;* Lockwood and McMillan 1971).

d) Light Curves in K (2.2 μ)

For most of the Mira variables discussed here, the wavelength 1.04 μ is close to the peak of the energy distribution at *maximum* light, when the spectral type is M5 or M6. At minimum light, however, the peak energy in these same stars has shifted to the 1.5–2.0-μ range. It is therefore of interest to compare the $I(104)$ curves with light curves measured closer to the energy maximum at minimum light. The K-magnitude of the standard wide-band multicolor system (Johnson 1966), with an effective wavelength of 2.2 μ, will serve this purpose.

Mendoza V. (1967) has compiled a catalog of observations of Mira variables on the standard system. Two stars—o Cet and χ Cyg—have a sufficient number of observations at different phases to show the character of their light curves at 2.2 μ. In Figure 7, the K-magnitudes of o Cet and χ Cyg are plotted against the phases computed from the light

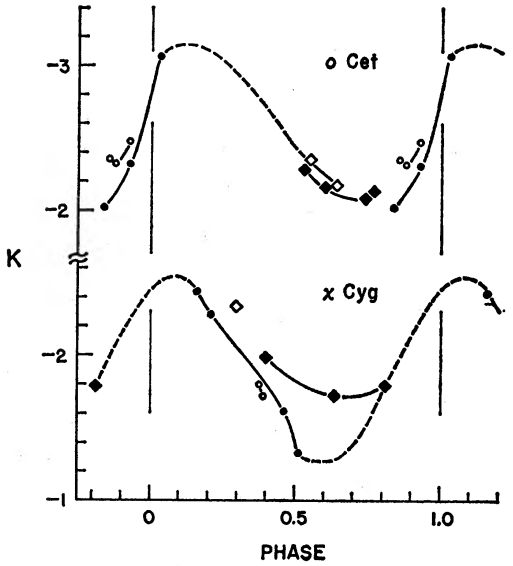

FIG. 7.—Light curves for o Cet (*upper*) and χ Cyg (*lower*) in the wide-band K-magnitude at 2.2 μ. Data from Mendoza V. (1967) are plotted against phases computed from the light elements of Table 2. Coded as in Fig. 1.

elements of Table 2. The correspondence between symbol and cycle number is the same as in the $I(104)$ curves for these stars shown in Figures 1 and 6, respectively. Measurements made within 3 days of one another have been averaged.

The K-curve for o Cet, as drawn, is very similar to the $I(104)$ curve in its amplitude ($\sim$1.1 mag), its lack of a hump on the rising branch, and its rather good repeatability. The phase of minimum in K is somewhat later than in $I(104)$, and the subsequent rise to maximum is steeper. The K-magnitude is not free from molecular absorption, and in late M stars the principal absorber is H_2O which acts to increase the amplitude by depressing the minimum of the light curve. The amplitude at a continuum point in the 2-μ region is thus probably not greater than 1.0 mag, or slightly less than the amplitude in $I(104)$.

The K-curve for χ Cyg shows large cycle-to-cycle differences, as does its $I(104)$ curve (Fig. 6), and the amplitude is not well defined. However, the series of four K observations of cycle 1 in 1965 (*filled circles*) was concurrent with a series in $I(104)$ which extended from a bright maximum to a faint minimum, so that the brightest and faintest measurements of K must be close to the extreme values, setting an upper limit to the mean amplitude in K of $\sim$1.3 mag. It is interesting that χ Cyg, which possesses the largest known ranges in V and $I(104)$, has a K range that is probably no larger, in a typical cycle, than that of o Cet. This result can be understood in terms of absorption in the K filter. Not only does χ Cyg at minimum have weaker H_2O bands than o Cet as a result of its lower oxygen-to-carbon ratio (Spinrad *et al.* 1966), but also the absorption by the CN molecule (Wing and Spinrad 1970), which is greatest at maximum light, is stronger in χ Cyg than in o Cet. Thus the net effect of CN and H_2O absorption within the K filter is to increase the amplitudes of M stars and to decrease the amplitudes of S stars. The first-overtone bands of CO also fall within this filter, but are relatively insensitive to phase.

IV. DISCUSSION

The gigantic loops executed by Mira variables in diagrams of molecular-band strength versus temperature (Wing 1967*c;* Spinrad and Wing 1969), and the fact that a given variable follows different paths in such diagrams in different cycles, indicate that the atmospheric layers producing the continuum and the molecular absorptions behave semi-independently. In the visual region, where the spectrum is broken by strong molecular

absorption features, the light we measure is coming from various layers, the relative contributions of which to the wide-band magnitude are constantly changing. It was perhaps not unreasonable to hope that by measuring nearly pure photospheric radiation throughout the cycle, as is done by the $I(104)$ magnitude, a simpler light curve would result. However, we have found that even the photospheric brightness variations are only semiregular in nature, and that infrared photometry does not lessen the need to observe Mira variables continually. Evidently, one should not expect more consistent behavior by such tenuous and distended atmospheres.

It is of some interest to look for systematic differences in the forms of the light curves of stars of types M and S. In addition to the four S stars, three of our stars (T Cas, T Cep, and S Her) may be called MS stars on the basis of the presence of weak ZrO bands (Spinrad and Newburn 1965; Keenan 1966; Wing 1967*c*).

It is intriguing that all three MS stars show substantial humps and that T Cas and T Cep have unusually small $I(104)$ amplitudes for their periods. On the other hand, there are no clear systematic differences in the shapes or amplitudes of the $I(104)$ curves between pure M and pure S stars, although the unidentified absorptions at faint phases in some stars with strong S characteristics (e.g., R Cyg) may introduce a systematically larger amplitude compared with M stars of the same bolometric amplitude. No complete $I(104)$ light curves have yet been obtained for carbon-type Miras, but from what is known about their mean visual light curves and Hetzler's (1936) photographic infrared curves, we would not expect their $I(104)$ curves to differ systematically from those of M or S stars.

One of our original objectives was to see if abnormally bright (and faint) visual maxima, in a given star, are also abnormally bright (and faint) in the infrared continuum. We find no simple answer to this question, for two separate phenomena appear to be involved. First, several variables have been observed to reach almost exactly the same maximum $I(104)$ magnitude in cycles that differed considerably in maximum visual magnitude. Examples of such behavior have been pointed out previously in the case of the normal (M7.0–M8.8) Mira variable W Peg (Wing 1967*c*) and the very cool Mira IK Tau (Spinrad and Wing 1969), and other examples can be found in the data of this paper (see, for example, our discussions of *o* Cet and S Her in §§ III*b* and III*c*, respectively). In these cases, earlier spectral types were recorded in the cycles that were brighter visually, but there is little evidence for important differences in the maximum temperature. The picture that emerges is that the photospheric temperature and bolometric magnitude probably go through similar variations in different cycles, but that different degrees of dissociation of TiO are reached in the upper atmosphere with resulting differences in blanketing in the visual region. Second, in other cases we have observed bright visual maxima that were also bright in $I(104)$, so that differences in spectral type cannot be the sole cause. The most striking examples of this behavior are χ Cyg and R Cas in Figure 6. In these cases, the temperatures estimated from the near-infrared energy distributions (Wing 1971*b*) were substantially higher at the brighter maxima, and the spectral type was abnormally early as well, so that an abnormally bright bolometric maximum is probably involved. In short, it seems that some bright visual maxima result from unusually high photospheric temperatures and bright bolometric magnitudes whereas others merely reflect a high degree of molecular dissociation in the upper atmosphere.

In a similar vein, we have attempted to interpret what is happening in the atmosphere when a Mira recovers from minimum light and especially when it goes through a hump on the rising branch of the light curve. The brightenings and humps are evidently unrelated to changes in spectral type, not only because $I(104)$ is free of blanketing but also because the spectral type stays practically constant, at its latest value for the cycle in question, from about phase 0.5 to about phase 0.7, regardless of whether or not a hump occurs during the interval. For example, the type of S Her in cycle 5 (*filled triangles* in

Fig. 4) remained at M8.0 while $I(104)$ brightened by 0.5 mag in 24 days in climbing from minimum to a pronounced secondary maximum. Likewise, observations of the rising branch of R Leo in three different cycles yielded three parallel but well-displaced branches, along each of which the spectral type remained constant. Although our temperatures are not well determined when the spectral types are later than M8.0, the sense of temperature changes can be ascertained with confidence from the observed changes in color, especially when the spectral type remains constant. We consistently find that the temperature increases steadily from the time of mimimum until visual maximum, again without regard for whether a hump occurs.

Pettit and Nicholson (1933) showed that the radius is decreasing throughout the rising branch, reaching a minimum value at phase 0.0. Since we have confirmed the phasing they found for the temperature and bolometric magnitude variations, we also concur, at least qualitatively, with their conclusions regarding the radius variation. In fact, the occasional occurrence of secondary maxima is strong evidence for a decrease in radius at late phases: our data show that the temperature continues to increase during the brief decline in light after secondary maximum, and this can happen only if the radius becomes smaller.

It is difficult to support the hypothesis that the humps on the rising branch are indicative of pulsation in the first overtone of the fundamental period, for the humps do not occur midway between the primary maxima, and in some stars they occur only occasionally. Rather, the humps seem to be merely the result of the interplay between rising temperature and decreasing radius during this part of the cycle.

We have attempted to account for a variety of observed features in the light curves of Mira variables in terms of changes in temperature, radius, and spectral type, but no attempt was made to explain the changes in the physical parameters themselves. The light curves suggest that an important event occurs near the time of minimum light, causing a sudden increase in photospheric temperature and the beginning of a new cycle. At minimum light, the atmosphere is saving energy, since losses by radiation are small; the crucial problem, it seems to us, is to identify the form of the energy stored at this time and to show how it is converted to the forms that are observed, both photometrically and spectroscopically, throughout the cycle until the next minimum. We hope that our observations will stimulate efforts to construct the dynamical models which ultimately will reveal the physical nature of the Mira phenomenon.

This project was made possible by generous allotments of telescope time at Lick Observatory and Kitt Peak National Observatory. Wing's observations were mostly made during the tenure of a Lick Fellowship, and he would like to acknowledge the advice and encouragement received from many members of Lick Observatory and the Berkeley Astronomy Department, and particularly from his thesis advisor, Dr. H. Spinrad. While this paper was being written, Wing was supported at the Ohio State University by a grant from the National Science Foundation. Lockwood would like to thank T. A. Zinter for his considerable help in reducing the Kitt Peak observations.

REFERENCES

Ahnert, P. 1964, *Mitt. Verh. Sterne* (Sonneberg), **2**, 66.
———. 1965, *ibid.*, **3**, 6.
Campbell, L. 1955, *Studies of Long-Period Variables* (prepared by M. W. Mayall for the American Association of Variable Star Observers).
Eggen, O. J. 1967, *Ap. J. Suppl.*, **14**, 307 (No. 131).
Evans, N. R. 1970, *A.J.*, **75**, 636.
Fernie, J. D. 1959, *Ap. J.*, **130**, 611.
Harrington, J. P. 1965, *A.J.*, **70**, 569.
Hayes, D. S. 1970, *Ap. J.*, **159**, 165.
Hetzler, C. 1936, *Ap. J.*, **83**, 372.

Johnson, H. L. 1966, *Ann. Rev. Astr. and Ap.*, **4**, 193.
Johnson, H. L., Mitchell, R. I., Iriarte, B., and Wiśniewski, W. Z. 1966, *Comm. Lunar and Planet. Lab.*, **4**, 99.
Keenan, P. C. 1957, *Pub. A.S.P.*, **69**, 5.
———. 1963, in *Basic Astronomical Data*, ed. K. Aa. Strand (Chicago: University of Chicago Press), p. 78.
———. 1966, *Ap. J. Suppl.*, **13**, 333 (No. 118).
Kukarkin, B. V., Kholopov, P. N., Efremov, Yu. N., Kukarkina, N. P., Kurochkin, N. E., Medvedeva, G. I., Perova, N. B., Fedorovich, V. P., and Frolov, M. S. 1969, *General Catalogue of Variable Stars* (3d ed.; Moscow: U.S.S.R. Academy of Sciences).
Landolt, A. U. 1969, *Pub. A.S.P.*, **81**, 134.
Lockwood, G. W. 1970, *Ap. J.* (*Letters*), **160**, L47.
———. 1971 (in preparation).
Lockwood, G. W., and McMillan, R. S. 1971, *Proceedings of the Conference on Late-Type Stars*, ed. G. W. Lockwood and H. M. Dyck (Tucson: Kitt Peak National Observatiory Contribution No. 554).
Mayall, M. W. 1964–1970, *Bulletin*, Nos. 27–33 (Cambridge, Mass.: American Association of Variable Star Observers).
Mendoza V., E. E. 1967, *Bol. Obs. Tonantzintla y Tacubaya*, **4**, 114.
Merrill, P. W. 1960, in *Stellar Atmospheres*, ed. J. L. Greenstein (Chicago: University of Chicago Press), p. 509.
Merrill, P. W., Deutsch, A. J., and Keenan, P. C. 1962, *Ap. J.*, **136**, 21.
Nassau, J. J. 1964, *Pub. A.S.P.*, **76**, 94.
Pettit, E., and Nicholson, S. B. 1933, *Ap. J.*, **78**, 320.
Pettit, M. S. 1944, *Pub. A.S.P.*, **56**, 107.
Schneller, H. 1965, *Mitt. Verh. Sterne* (Sonneberg), **3**, 86.
Sky and Telescope. 1969, **38**, 223.
Smak, J. I. 1964, *Ap. J. Suppl.*, **9**, 141 (No. 89).
———. 1966, *Ann. Rev. Astr. and Ap.*, **4**, 19.
Spinrad, H., and Newburn, R. L., Jr. 1965, *Ap. J.*, **141**, 965.
Spinrad, H., Pyper, D. M., Newburn, R. L., and Younkin, R. L. 1966, *Ap. J.*, **143**, 291.
Spinrad, H., and Wing, R. F. 1969, *Ann. Rev. Astr. and Ap.*, **7**, 249.
Turner, B. E., Buhl, D., Churchwell, E. B., Mezger, P. G. and Snyder, L. E. 1970, *Astr. and Ap.*, **4**, 165.
Wilson, W. J., Barrett, A. H., and Moran, J. M. 1970, *Ap. J.*, **160**, 545.
Wing, R. F. 1967*a*, *Colloquium on Late-Type Stars*, ed. M. Hack (Trieste: Osservatorio Astronomico di Trieste), p. 205.
———. 1967*b*, *ibid.*, p. 231.
———. 1967*c*, unpublished Ph.D. thesis, University of California, Berkeley.
———. 1971 (in preparation).
Wing, R. F., and Spinrad, H. 1970, *Ap. J.*, **159**, 973.
Wing, R. F., Spinrad, H., and Kuhi, L. V. 1967, *Ap. J.*, **147**, 117.
Wyckoff, S. 1970, *Ap. J.*, **162**, 203.